Relativistic description of the $np \to \eta d$ reaction near threshold

H. Garcilazo[1] and M. T. Peña[2]

[1] *Escuela Superior de Física y Matemáticas Instituto Politécnico Nacional, Edificio 9, 07738 México D.F., Mexico*

[2] *Instituto Superior Técnico, Centro de Física das Interacções Fundamentais, and Department of Physics, Av. Rovisco Pais, 1049-001 Lisboa, Portugal*

(Dated: February 8, 2008)

arXiv:nucl-th/0406070v1 22 Jun 2004

Abstract

Relativistic effects in a three-body calculation of the $np \to \eta d$ process are considered. Relativistic effects on the range and strength of the pion exchange contribution to the reaction mechanism may be large, but boost effects of the two-body interactions are negligible. The relativistic calculation confirms previous non-relativistic results, showing that the shape of the cross section near threshold is essentially determined by the ηd final-state interaction alone. As for the region away from threshold, the relativistic pion exchange contribution is seen to dominate the other mechanisms of the reaction. It turns out that, within the relativistic reaction model, the $np \to \eta d$ experimental data excludes large values for the real part of the ηN scattering length.

PACS numbers: 21.30.Fe, 21.45.+v,25.10.+s,11.80.Jy

I. INTRODUCTION

We investigate relativistic effects in the reaction $np \to \eta d$, in a calculation that considers the ηd final state three-body distortion. The inclusion of this interaction is crucial for the interpretation of the observed behavior of the cross-section at threshold [1, 2]. In previous works [3, 4, 5] we concluded that the shape of the cross-section very near threshold is indeed determined by the three-body nature of the final state interaction. Those calculations were however made within a non-relativistic formalism, with the only addition of non-relativistic kinematics for the pion. Here we introduce and solve a relativistic formalism with the following features:

i) On one hand, covariant meson-nucleon amplitudes based on different data analyses [6, 7, 8, 9, 10] of the coupled reactions $\pi N \to \eta N$, $\eta N \to \eta N$ and $\gamma N \to \eta N$ are constructed for the first time. The covariant meson-nucleon amplitudes are moreover conveniently boosted (including their Dirac spin structure) to be embedded in the meson production mechanism through which the reaction proceeds. This mechanism is the meson-exchange box diagram with the excitation of the S_{11} resonance, represented in Fig. 1. ii) On the other hand, for the calculation of the ηd final state distortion, a relativistic version of the 3-body equations is used, which incorporates relativistic kinematics and the boost of the two-body interactions. This last effect for the meson-nucleon interactions is also studied.

There is a considerable dispersion of the empirical values for the ηN scattering originated by different data analysis [6, 7, 8, 9, 10]. The inclusion of relativity in the calculation of the $np \to \eta d$ cross section is needed to narrow the large uncertainty region for that scattering length. In the light of the relativistic description used here, the width of this region is seen to be narrowed.

The next section describes the formalism: in Section 2.A the relativistic meson-exchange driving term is introduced and in Section 2.B the three-body relativistic formalism for the ηd final state interaction is addressed. In section III the results are shown and discussed. Section IV summarizes the conclusions.

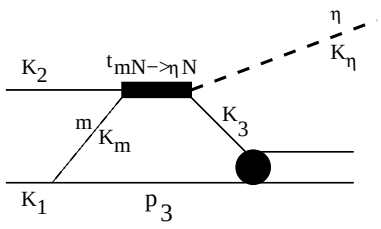

FIG. 1: Meson-exchange mechanism for the reaction $np \to \eta d$

II. FORMALISM

A. The Covariant $np \to \eta d$ Box Diagram

We will start our discussion with the box diagram shown in Fig.1, which together with the impulse term, has been considered as the basic meson production mechanism [4, 5, 11, 12, 13].

If one evaluates this Feynman diagram by putting the spectator nucleon on-the-mass-shell one obtains

$$A_{M_d}^{\mu_1\mu_2} = \frac{1}{(2\pi)^3}\sum_{\mu}\int d\vec{p}_N \quad \frac{M}{E_N}\bar{v}_N^{\mu}V_{dNN}^{M_d}\frac{\not{p}_3+M}{p_3^2-M^2}t_{mN\to\eta N}u_2^{\mu_2} \times\frac{1}{k_m^2-m_m^2}\bar{u}_N^{\mu}V_{mNN}u_1^{\mu_1}, \tag{1}$$

where $V_{dNN}^{M_d}$, V_{mNN} and $t_{mN\to\eta N}$ are respectively, the deuteron-nucleon-nucleon vertex, the m meson-nucleon-nucleon vertex, and the meson-nucleon $\to \eta$ nucleon t-matrix. The spinors $u_1^{\mu_1}$, $u_2^{\mu_2}$, u_N^{μ}, correspond respectively the two initial and the intermediate nucleon spinors, and $\bar{v}_N^{\mu}$ is the charged-conjugated spinor. The 3-momentum variables are defined as shown on the diagram of Fig. 1.

One expects the effect of relativity to be important in the left hand-side of the box diagram where the exchanged meson m is very far-off-the-mass-shell. However, on the right-on-side of the diagram the final η is restricted to the energy region of $E < 100$MeV, so that the effects of relativity are not so crucial. Therefore, we will write the propagator for the intermediate nucleon in terms of positive and negative energy spinors and keep only the positive energy part:

$$\frac{\not{p}_3+M}{p_3^2-M^2} = \frac{M}{E_3}\sum_{\mu_3}\frac{u_3^{\mu_3}(\vec{p}_3)\bar{u}_3^{\mu_3}(\vec{p}_3)}{p_{03}-E_3} + \frac{M}{E_3}\sum_{\mu_3}\frac{v_3^{\mu_3}(-\vec{p}_3)\bar{v}_3^{\mu_3}(-\vec{p}_3)}{p_{03}+E_3}$$

$$\rightarrow \frac{M}{E_3}\sum_{\mu_3}\frac{u_3^{\mu_3}(\vec{p}_3)\bar{u}^3_{\mu_3}(\vec{p}_3)}{p_{03}-E_3} \tag{2}$$

If we now consider the deuteron wavefunction $\Psi^*_{M_d,\mu\mu_3}(\vec{p}\,)$ defined by the identification [14]

$$\frac{M}{E_3}\bar{v}^{\mu}_N(\vec{k}_3)V^{M_d}_{dNN}u_3^{\mu_3}(\vec{p}_3)\frac{1}{p_{03}-E_3} \equiv \sqrt{2\omega_d}(2\pi)^{3/2}\Psi^*_{M_d,\mu\mu_3}(\vec{p}\,) \tag{3}$$

where $\vec{p}$ is the NN relative momentum in the center of mass, we obtain from Eq.(1)

$$A^{\mu_1\mu_2}_{M_d} = \frac{1}{(2\pi)^{3/2}}\sum_{\mu,\mu_3}\int d\vec{p}_N \quad \frac{M}{E_N}\sqrt{2\omega_d}\Psi^*_{M_d,\mu\mu_3}(\vec{p}\,)\bar{u}_3^{\mu_3}(p_3)t_{mN\rightarrow\eta N}u_2^{\mu_2}(p_2)$$
$$\times\frac{1}{p_m^2-m_m^2}\bar{u}^{\mu}_N(p_N)V_{mNN}u_1^{\mu_1}(p_1). \tag{4}$$

In Eq. 4 we made explicit the momentum dependence of the nucleon spinors.

The deuteron wavefunction is on the other hand calculated from

$$\Psi^*_{M_d,\mu\mu_3}(\vec{p}\,) = \sum_{L=0,2}\sum_{m_L,m_S} C^{L\ 1\ 1}_{m_L\ m_S\ M_d}\ \phi_L(p)Y^*_{Lm_L}(\hat{p})\ C^{1/2\ 1/2\ 1}_{\mu\ \ \mu_3\ \ m_S}, \tag{5}$$

where $\phi_0(p)$ and $\phi_2(p)$ are the S- and D-wave components which we obtained from the Paris potential.

For the m meson-nucleon-nucleon vertex we take

$$V_{mNN} = g_m\gamma_5 f_m(k_m^2),\ \ m=\pi,\eta \tag{6}$$

and

$$V_{mNN} = g_m f_m(k_m^2),\ \ m=\sigma \tag{7}$$

where k_m^2 is the meson four-momentum squared and the form factor f_m is chosen to have the monopole form

$$f_m(k_m^2) = \frac{\Lambda^2-m_m^2}{\Lambda^2-k_m^2} \tag{8}$$

with $\Lambda = 1800$ MeV/c.

Since the η production near threshold is dominated by the S_{11} resonance, the m meson-nucleon $\rightarrow$ η-nucleon t transition operator is assumed to be generated by a variable mass isobar model consisting of a single isobar, the S_{11}. As in the framework introduced in ref.[15] for the study of the pion induced eta production reaction, the isobar model for meson-nucleon scattering used here is covariant, and reads:

$$t_{mN\rightarrow\eta N}(\vec{p}^{\,2},\vec{p}^{\,\prime 2},M_S) \ = \ \frac{(2\pi)^2}{M}\sqrt{\omega_m(\vec{p}^{\,2})\omega_\eta(\vec{p}^{\,\prime 2})E_N(\vec{p}^{\,2})E_N(\vec{p}^{\,\prime 2})}$$
$$\times h_m(\vec{p}^{\,2})\frac{\not{k}_N + \not{k}_2 + M_S}{2M_S}h_\eta(\vec{p}^{\,\prime 2})\tau(M_S) \tag{9}$$

where $\omega_m(\vec{p}^{\,2}) = \sqrt{m_m^2 + \vec{p}^{\,2}}$, $E_N(\vec{p}^{\,2}) = \sqrt{M^2 + \vec{p}^{\,2}}$ are the on-shell energies respectively of the m meson and of the nucleon in the c.m. frame. Also one has

$$M_S = \sqrt{(k_m + k_2)^2} = \sqrt{(k_\eta + k_3)^2}. \tag{10}$$

The meson-nucleon-isobar vertices are

$$h_m(\vec{p}^{\,2}) = \sqrt{\frac{2M}{M + E_N(\vec{p}\,)}} g_m(\vec{p}^{\,2}), \;\; m = \pi, \eta \tag{11}$$

and

$$h_m(\vec{p}^{\,2}) = \frac{M}{\sqrt{\vec{p}^{\,2}}} \sqrt{\frac{2M}{M + E_N(\vec{p}\,)}} g_m(\vec{p}^{\,2})\gamma_5, \;\; m = \sigma \tag{12}$$

Here, three-momentum squared $\vec{p}^{\,2}$ ($\vec{p}^{\,\prime 2}$) is the meson-nucleon relative initial (final) three-momentum in the c.m frame. In particular, it is related to Lorentz invariant quantities as

$$\vec{p}^{\,2} = \frac{(M_S^2 + M^2 - k_m^2)^2}{4M_S^2} - M^2. \tag{13}$$

The isobar propagator $\tau(M_S)$ is obtained from a separable potential model describing the coupled $\eta N - \pi N - \sigma N$ two-body subsystem. The corresponding two-body $t-$matrix (9) is also separable in any reference frame. We note that the σN channel stands for the $\pi\pi N$ inelasticity. Also, in variance with refs. [16] we do not consider ρ-exchange. Recently in ref. [12] it is shown that the exact numerical treatment of the initial state interaction reduces significantly the ρ-exchange diagram, relatively to the other meson exchanges.

The matrix element of the transition operator on Eq. (9) in the 2 body meson-nucleon c.m. system, where $\vec{k}_m + \vec{k}_2 = \vec{k}_\eta + \vec{k}_3 = 0$, in the basis states of the nucleon spinors is given by

$$\begin{aligned} \bar{u}_3^{\mu_3} t_{mN\to\eta N} u_2^{\mu_2} \;\; = \;\; & \frac{2\pi}{M} \delta_{\mu_2\mu_3} \sqrt{\omega_m(\vec{p}^{\,2})\omega_\eta(\vec{p}^{\,\prime 2}) E_N(\vec{p}^{\,2}) E_N(\vec{p}^{\,\prime 2})} \\ & \times g_m(\vec{p}^{\,2}) \tau(M_S) g_\eta(\vec{p}^{\,\prime 2}). \end{aligned} \tag{14}$$

We consider nucleon 2 with momentum $\vec{q}_N$ in the positive direction of the z-axis and the η meson 3-momentum in the xz plane with polar angle θ. Then the amplitude $\mathcal{A}$ of Eq. (4) satisfies the symmetry property

$$A_M^{\mu_1\mu_2}(\vec{q}_N, \theta) = -(-1)^{M+\mu_1+\mu_2} A_M^{\mu_1\mu_2}(-\vec{q}_N, \pi - \theta). \tag{15}$$

In the isospin formalism the neutron and proton are identical particles, so that the initial np state must be antisymmetrized under the exchange of nucleons 1 and 2. However,

the system is in a pure total isospin 0 state, which means that the initial np state must be symmetric under the exchange of space and spin variables. Therefore, the correctly antisymmetrized amplitude $\bar{A}_M^{\mu_1\mu_2}$ for the $np \to \eta d$ process is

$$\begin{aligned} \bar{A}_M^{\mu_1\mu_2} &= \frac{1}{\sqrt{2}} \left[A_M^{\mu_1\mu_2}(\vec{q}_N, \theta) + A_M^{\mu_2\mu_1}(-\vec{q}_N, \theta) \right] \\ &= \frac{1}{\sqrt{2}} \left[A_M^{\mu_1\mu_2}(\vec{q}_N, \theta) - (-1)^{M+\mu_1+\mu_2} A_M^{\mu_2\mu_1}(\vec{q}_N, \pi - \theta) \right]. \end{aligned} \tag{16}$$

B. The ηd scattering and the boost of the two-body interactions

In our previous work [5] we presented the formalism of ηd elastic scattering based on nonrelativistic Faddeev equations. Since we are now discussing relativistic effects in the $np \to \eta d$ process, it becomes necessary to perform here also a relativistic calculation of the ηd elastic channel responsible for the final-state interaction in the $np \to \eta d$ reaction. To generate the necessary ηd distorted waves, we apply to the ηd elastic channel the relativistic formalism in momentum space presented in Ref. [17]. This formalism generalizes in a straightforward way the non-relativistic Faddeev equations. It incorporates relativistic kinematics and, importantly, also the boosts of the two-body interactions to the three-body c.m. frame

Firstly, the main feature of the formalism of [17] is to consist of a set of relativistic but 3-dimensional integral Faddeev-type equations obtained from a field theory in which the three particles are kept on their mass shells in all intermediate states. Accordingly, in what follows the quantity k_i does not refer to the four-momentum of particle i, but to the magnitude of the 3-momentum $\vec{k}_i$. Secondly, in order to transform correctly all physical quantities from the two-body to the three-body reference frames, and after considering the energy conservation constraint, one writes the invariant momentum space volume element for the three particles in terms of the two relative Jacobi variables $\vec{p}_i$ and $\vec{q}_i$,

$$\begin{aligned} d\mathcal{V} &= \frac{d\vec{k}_1}{2\omega_1(k_1)} \frac{d\vec{k}_2}{2\omega_2(k_2)} \frac{d\vec{k}_3}{2\omega_3(k_3)} \delta(\vec{k}_1 + \vec{k}_2 + \vec{k}_3) \\ &= \frac{\omega(p_i)}{8W_i(p_i q_i)\omega_i(q_i)\omega_j(p_i)\omega_k(p_i)} d\vec{p}_i d\vec{q}_i, \end{aligned} \tag{17}$$

The variable $\vec{p}_i$ is the relative momentum of the pair jk measured in the c.m. frame of the pair (that is, the frame in which particle j has momentum $\vec{p}_i$ and particle k has momentum $-\vec{p}_i$), and $\vec{q}_i = -\vec{k}_i$ is the relative momentum between the pair jk and the spectator particle i,

measured in the c.m. frame of the three particles, (in which the pair jk has total momentum $\vec{q}_i$ and particle i has momentum $-\vec{q}_i$). The energy of the jk pair in its c.m. frame is

$$\omega(p_i) = \sqrt{m_j^2 + p_i^2} + \sqrt{m_k^2 + p_i^2}, \tag{18}$$

the total energy of the pair is

$$W_i(p_i q_i) = \sqrt{\omega^2(p_i) + q_i^2}, \tag{19}$$

and the invariant energy of the three particles is written

$$W(p_i q_i) = \omega_i(q_i) + W_i(p_i q_i). \tag{20}$$

Equations (17) throughout (20) determine the transformation of the matrix elements of the two-body potential V from the two-body to the three-body reference frames as in [17]

$$\begin{aligned} < \vec{p}_i \vec{q}_i | V | \vec{p}_i' \vec{q}_i' > \; = \; & \left[\frac{W_i(p_i q_i)\omega_j(p_i)\omega_k(p_i) W_i(p_i' q_i)\omega_j(p_i')\omega_k(p_i')}{\omega(p_i)\omega(p_i')} \right]^{1/2} \\ & \times 8\omega_i(q_i)\delta(\vec{q}_i - \vec{q}_i')V(\vec{p}_i, \vec{p}_i'), \end{aligned} \tag{21}$$

which in turn defines the boosted matrix elements of the two-body t-matrix. These are given by

$$\begin{aligned} < \vec{p}_i \vec{q}_i | t | \vec{p}_i' \vec{q}_i' > \; = \; & \left[\frac{W_i(p_i q_i)\omega_j(p_i)\omega_k(p_i) W_i(p_i' q_i)\omega_j(p_i')\omega_k(p_i')}{\omega(p_i)\omega(p_i')} \right]^{1/2} \\ & \times 8\omega_i(q_i)\delta(\vec{q}_i - \vec{q}_i')t(\vec{p}_i, \vec{p}_i'; q_i), \end{aligned} \tag{22}$$

where $t(\vec{p}_i, \vec{p}_i'; q_i)$ satisfies the Lippmann-Schwinger equation with a propagator corresponding to relativistic kinematics defined by Eq. (20):

$$\begin{aligned} t(\vec{p}_i, \vec{p}_i'; q_i) \; = \; & V(\vec{p}_i, \vec{p}_i') + \int d\vec{p}_i'' V(\vec{p}_i, \vec{p}_i'') \\ & \times \frac{1}{W_0 - W(p_i'' q_i) + i\epsilon} t(\vec{p}_i'', \vec{p}_i'; q_i). \end{aligned} \tag{23}$$

The variable W_0 is the invariant energy of the system. For only S-wave two-body interactions Eq. (23) becomes

$$\begin{aligned} t(p_i, p_i'; q_i) \; = \; & V(p_i, p_i') + \int_0^\infty p_i''^2 dp_i'' V(p_i, p_i'') \\ & \times \frac{1}{W_0 - W(p_i'' q_i) + i\epsilon} t(p_i'', p_i'; q_i). \end{aligned} \tag{24}$$

In the particular case of the coupled $\eta N - \pi N - \sigma N$ subsystem (we take $m_\sigma = 2m_\pi$, since the σN channel simulates the $\pi\pi N$ inelasticity), these three different meson-nucleon channels are connected among each other through the S_{11} partial wave. For each transition, we use rank-one separable potentials of the form

$$V_{mm'}(p_i, p_i') = -g_m(p_i) g_{m'}(p_i'); \qquad (m, m' = \eta, \pi, \sigma) \tag{25}$$

where the functions g_m are as in ref. [5],

$$g_m(p_i) = \sqrt{\lambda_m} \frac{A_m + p_i^2}{(\alpha_m^2 + p_i^2)^2}; \qquad (m = \eta, \pi) \tag{26}$$

$$g_m(p_i) = \sqrt{\lambda_m} \frac{p_i}{(\alpha_m^2 + p_i^2)^2}; \qquad (m = \sigma) \tag{27}$$

so that the solution of Eq. (24) is

$$t_{mm'}(p_i, p_i'; q_i) = g_m(p_i) \tau(q_i) g_{m'}(p_i'), \tag{28}$$

with

$$\tau^{-1}(W_0, q_i) = -1 - \sum_{m=\eta,\pi,\sigma} \int_0^\infty p_i^2 dp_i \frac{g_m^2(p_i)}{W_0 - W(p_i q_i) + i\epsilon}. \tag{29}$$

We will now make the connection between the boosted two-body t-matrix elements and the ones introduced in the previous section. For that, we take Eq. (22) in the two-body c.m. frame, where $q_i = 0$, and obtain

$$\begin{aligned} < \vec{p}_i \vec{0} | t | \vec{p}_i' \vec{q}_i' > \; &= \; [\omega_j(p_i)\omega_k(p_i)\omega_j(p_i')\omega_k(p_i')]^{1/2} \\ &\times 8 m_i \delta(\vec{0} - \vec{q}_i') t(\vec{p}_i, \vec{p}_i'; 0), \end{aligned} \tag{30}$$

We verify this way that the t-matrix given by Eq.(30), and generated by our separable potential model on Eq.(25), is proportional to Eq.(14). The different multiplicative factors come from normalization conventions for the two body momentum basis states, taken differently in relativistic and non-relativistic Faddeev-type formalisms.

The driving terms of the Faddeev equations for ηd elastic scattering given by Eqs. (20)-(22) of Ref. [5] are here modified by the inclusion of relativistic kinematics and an invariant three-body volume element by making the replacement

$$\begin{aligned} \frac{1}{E - p_j^2/2\mu_j - q_j^2/2\nu_j + i\epsilon} \; \rightarrow \; &\left[\frac{W_i(p_i' q_i)\omega_j(p_i')\omega_k(p_i') W_j(p_j q_j)\omega_k(p_j)\omega_i(p_j)}{\omega(p_i')\omega(p_j)\omega_i(q_i)\omega_j(q_j)} \right]^{1/2} \\ &\times \frac{1}{\omega_k(q_k)} \frac{1}{W_0 - W(p_j q_j) + i\epsilon}. \end{aligned} \tag{31}$$

with p_i', p_j, and $\omega_k(q_k)$ defined by Eqs. (70), (71), and (66) of Ref. [17].

In the case of the NN interaction for the intermediate re-sacttering series given in [5] by eqs. (19) and (20), and represented therein on Fig. 2, we used in [5] the PEST separable model of Ref.[18], which is based in the nonrelativistic Lippmann-Schwinger equation. Here, in order to make this interaction consistent with the relativistic Lippmann-Schwinger equation given by eq. (24) we re-adjusted numericaly the strength of the potential such that the deuteron pole appears at the right position. This amounts to multiplying the original PEST potential of Ref. [18] by the factor 0.78805. As for the ηNN coupling constant, it was given the reasonable value [19, 20, 21, 22, 23] $g_\eta^2/4\pi = 1$ while for the σNN coupling constant we used the value of Ref. [24] $g_\sigma^2/4\pi = 8$.

III. RESULTS

We give in table I the parameters of the seven models corresponding to the description of the meson-nucleon amplitude analyses of Refs. [6, 7, 8, 9, 10] by eqs. (24)-(28). The agreement of the amplitudes obtained with those analyses is at least as good as the ones shown in Fig. 1 in ref. [5], and therefore we do not show here the corresponding figure.

In all, to the exception of model 0, the parameters for σ-exchange are the ones that deviate less from the parameters obtained in ref. [5] from a non-relativistic calculation. However, due to its small mass, the pion contribution is affected by the relativistic treatment. In models 2-6 relativity increases slightly the momentum range parameter α_π. However, the strength parameter A_π increases also. Since, as seen from Eq.(26), it defines the weight of the small versus the large momentum region, this way it compensates the extra weight of the high momentum tail originated by the increase of the range. As for the ηN channel, the changes in the two parameters also balance out.

Models 1, and specially model 0, which correspond to smaller values for the ηN scattering lenghts, behave differently than the others, since the pion range is seen to decrease. Moreover, for model 0 the pion low-momentum strength A_π uniquely decreases more than the range parameter α_π. As a net result the weigth of the high momentum range versus the low momentum range is increased. This relative weight of small and large momenta reflects then on the behavior of the cross-section for $np \to \eta d$, as we will see below. The difference in behavior of model 0 may be due to the inclusion of ρ-exchange in the meson-nucleon

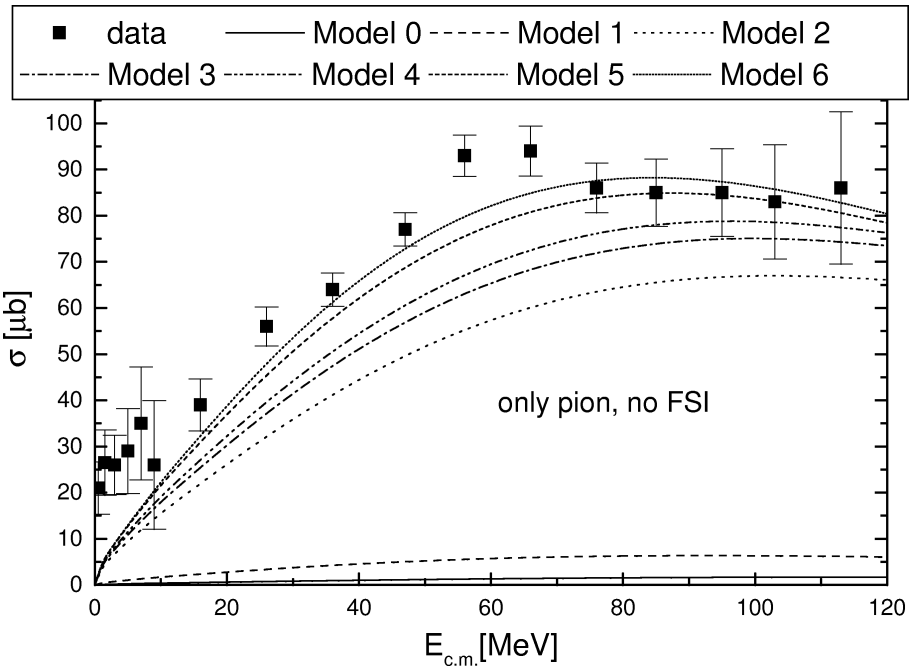

FIG. 2: Total cross section of the reaction $np \rightarrow \eta d$ for the seven relativistic meson-nucleon interaction models considered. Only pion exchange is considered in the box diagram represented by Fig. 1. No ηd final state interaction included. Data from refs. [1] and [2].

amplitude as explained in ref. [12], which has the role of counteracting the high momenta contribution of pion exchange.

We will turn now to the results obtained for the ηd three-body elastic channel. We give in table II the predictions for the three-body ηd scattering length obtained using the seven two-body ηN-πN-σN coupled interaction models. We present the results corresponding to the box diagram or driving term of the Faddeev equations (see Fig. 2 of Ref. [5]) including the different meson-exchanges, one by one, in successive cumulative steps: only η exchange, $\eta + \pi$ exchange or $\eta + \pi + \sigma$ exchange. To conclude about the extent of the relativistic effects we show for each model the non-relativistic results of [5] (lines labeled "NR"). The effect of the relativistic treatment on the three-body scattering length can be seen clearly in the contribution of the pion, which is the lightest meson. Its contribution to the 3 body scattering length is negligible in all non-relativistic models [5]. Compared with the corresponding results of [5], the relativistic results are still quite similar to those of the nonrelativistic case, to the exception of model 0. The pion exchange contribution to the scattering length is now quite important in the case of this model. This happens

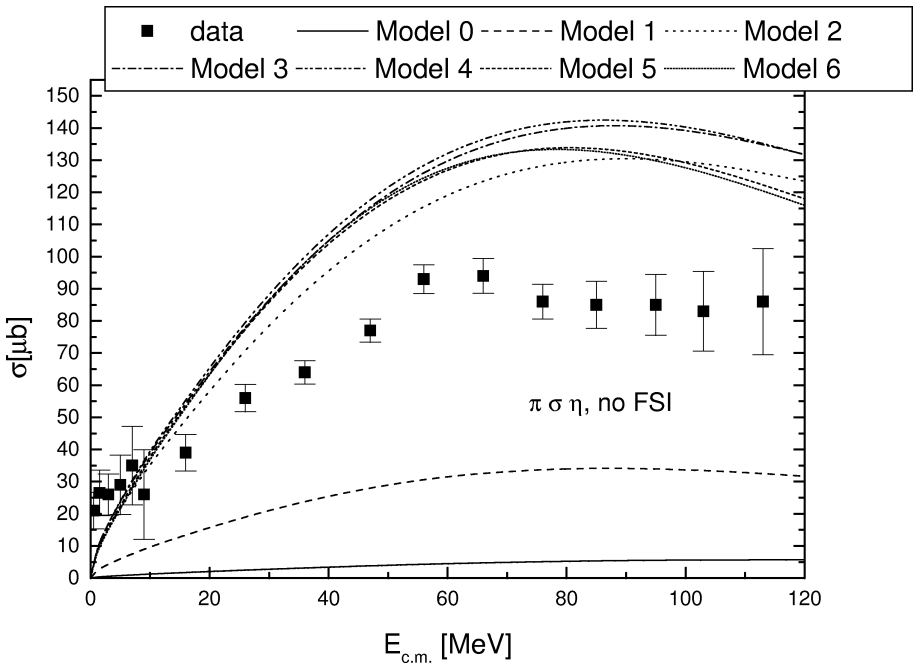

FIG. 3: The same as Fig.2 but with inclusion of π, η and σ exchanges in the diagram represented by Fig.1.

because in model 0, contrarily to the other models, the relativistic changes in the range α_π and low-momentum strength A_π parameters are not balanced, as in the other models.

Besides the changes that the relativistic two-body models induce in the pion exchange contribution, the comparison done on table II gives also indirect information on the magnitude of the boosts of the two body interactions within the 3-body system. Given the agreement observed in most cases between the relativistic and non-relativistic models, boost effects do not appear relevant. Since the energies involved ($\sim$ 100 MeV), are much smaller than the masses of the η and the nucleon, this is expected.

We show in Fig. 2 the cross section of the $np \to \eta d$ process when only pion exchange is included in the box diagram (see Fig. 1) and **no** final-state interaction is included. We considered a reduction factor of 5 corresponding to the initial-state interaction [5]. Although some of the models (those with a large ηN scattering length) predict more or less the right magnitude for the cross section at large energies, near threshold they all fail to reproduce the enhancement shown by the data. We notice that the models with larger relative low-momentum strength parameter A_π, larger absolute pion strength λ_π and smaller absolute η strength λ_η , are closer to the data away from threshold, where indeed only small momentum

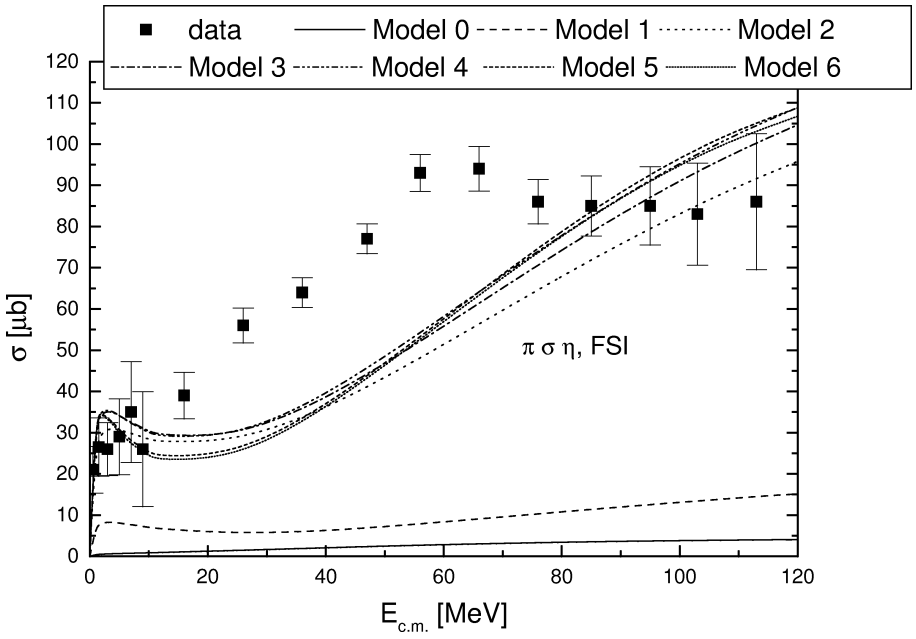

FIG. 4: The same as Fig.3 but with the inclusion of ηd final state interaction.

transfer is needed.

We show in Fig. 3 the corresponding results when in addition the contribution of the exchanges of the η and σ mesons are included in the box diagram. From both Figs. 2 and 3 it is clear that the dominant exchange mechanism for the $np \to \eta d$ process is pion exchange. This conclusion was also found by the substantially different calculations of refs. [12, 25].

We consider next the situation with regard to the final ηd distortion of the $np \to \eta d$ process. We show in Fig. 4 the results when in addition one includes the final-state interaction. The models with a large ηN scattering length give a good description of the data near threshold. This was already the case for the non-relativistic case in ref. [5] (see fig. 6 therein). The new feature of the relativistic calculation is that the high-energy end is now described by those models. However, they fail to reproduce the shape of the cross section in the intermediate region. The good description of the cross section at the high energy end by models 2-6 is due to the modification of the range and strength parameters for the pion in the dynamical two-body models - and does not happen for models 0 and 1.

Finally, we introduced in the box diagram the contribution of the η' meson with coupling constants adjusted so as to reproduce the cross section near threshold. Since this is a heavy meson exchange, this process acts like a background correction to the isobar model of the nucleon-meson amplitude. We show the results in Fig. 5. This figure is indicative that a

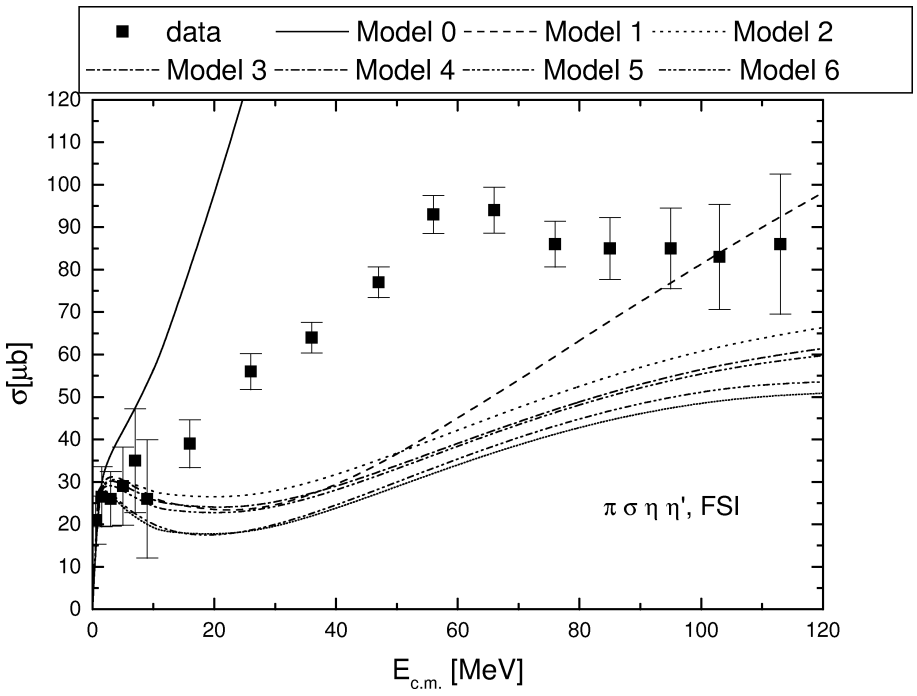

FIG. 5: The same as Fig. 4 but with the inclusion of η' exchange in the box diagram represented by Fig. 1.

reasonable description of the data could be obtained with a model in between model 0 and model 1, i.e., with a ηN scattering length larger than 0.42 fm and smaller than 0.72 fm. A finer tuning beyond this point demands an exact treatment of the initial state reduction effect, which as explained in ref [12], may be different for the different meson exchanges.

IV. CONCLUSIONS

To summarize, a relativistic calculation of the $np \to \eta d$, based on meson exchange production mechanisms, confirms that the final state ηd interactions is very important near threshold, as found before in non-relativistic models. This interaction alone explains the enhancement effect observed in the cross section near threshold.

Although the pion exchange visibly does not describe the data near threshold, an important conclusion is that the relativistic pion exchange contribution dominates the reaction exchange mechanisms. Moreover, it describes the high energy end of the measured cross-section, which was not the case for the non-relativistic version.

Finally, relativistic models corresponding to relatively lower values of the ηd scattering

length, e.g. the Julich model, when compared to their non-relativistic counterparts, have the pion strength in the large momentum tail accentuated relatively to the small momentum region. Simultaneously, however, the overall pion strength is reduced. These two features seem to be needed to describe successfully the energy dependence of the cross-section, in the threshold region, as well as away from the threshold energy region.

The control of relativistic effects are therefore important in phenomenological analysis of the reaction. Namely, it narrows considerably the uncertainty in the knowledge of the ηN scattering length. A value for this one between 0.42 fm and 0.72 fm seems to be indicated by this study.

This work was supported in part by COFAA-IPN (México) and by Fundação para a Ciência e a Tecnologia, under contract POCTI/FNU/50358/2002.

---

[1] H. Calén *et al.*, Phys. Rev. Lett. **79**, 2642 (1997).

[2] H. Calén *et al.*, Phys. Rev. Lett. **80**, 2069 (1998).

[3] H. Garcilazo and M. T. Peña, Phys. Rev. C **61** 064010 (2000).

[4] H. Garcilazo and M. T. Peña, Phys. Rev. C **63** 021001 (2001).

[5] H. Garcilazo and M. T. Peña, Phys. Rev. C **66** 034606 (2002).

[6] M. Batinić, I. Šlaus, A. Švarc, and B. M. K. Nefkens, Phys. Rev. C **51**, 2310 (1995).

[7] M. Batinić, I. Dadić, I. Šlaus, A. Švarc, B. M. K. Nefkens, and T.-S. H. Lee, Physica Scripta **58**, 15 (1998).

[8] A. M. Green and S. Wycech, Phys. Rev. C **55**, R2167 (1997).

[9] A. M. Green and S. Wycech, Phys. Rev. C **60**, 035208 (1999).

[10] A. Sibirtsev, S. Schneider, Ch. Elster, J. Haidenbauer, S. Krewald, and J. Speth, Phys. Rev. C **65**, 044007 (2003).

[11] W. Grein, A. König, P. Kroll, M. P. Locher, and A. Švarc, Ann. Phys. **153**, 301 (1984).

[12] V. Baru, A.M. Gasparian, J. Haidenbauer, C. Hanhart, J. Speth, A.E. Kudryavtsev and J. Speth, Phys.Rev.C **67** 024002,(2003).

[13] C. Hanhart, hep-ph/0311341

[14] W. W. Buck and F. Gross, Phys. Rev. D **20**, 2361 (1979).

[15] H. Garcilazo and M. T. Peña, Phys. Rev. C **59**, 2389 (1999).

[16] J-F. Germond and C. Wilkin, Nucl. Phys. **A518** 308 (1990); G.Fäldt and C. Wilkin, Phys. Scr. **64**, 427 (2001).

[17] H. Garcilazo, Phys. Rev. C **67**, 055203 (2003).

[18] H. Zankel, W. Plessas, and J. Haidenbauer, Phys. Rev. C **28**, 538 (1983).

[19] R. Machleidt, Adv. Nucl. Part. Phys. **19**, 189 (1989).

[20] T. Rijken and V. G. J. Stoks, Phys. Rev. C **59**, 21 (1999).

[21] M. Benmerrouche and N. C. Mukhopadhyay, Phys. Rev. Lett. **67**, 1070 (1991).

[22] L. Tiator, C. Bennhold, and S. S. Kamalov, Nucl. Phys. **A580**, 455 (1994).

[23] Shu-Lin Zhu, Phys. Rev. C **61**, 065205 (2000).

[24] K. Holinde, Phys. Reports **68**, 121 (1981).

[25] K. Nakayama, J. Speth, and T.-S. H. Lee, Phys. Rev. C **65**, 045210 (2002).

TABLE I: Parameters of the ηN-πN separable potential models fitted to the S_{11} resonant amplitudes given in Refs. [7-10].

Model	Ref.	$a_{\eta N}$	α_η	A_η	λ_η	α_π	A_π	λ_π	α_σ	λ_σ
0	[10]	0.42+i0.34	5.85798	7.20057	-202.573	0.384338	0.00306689	-0.0804278	0.808	-0.155061
1	[7]	0.72+i0.26	29.9983	359.211	-5991.79	2.28053	1.08638	-0.0660518	8.0	-239.860
2	[8]	0.75 + i0.27	6.80695	409.632	-0.0735564	9.17614	1.46599	-701.087	8.0	-816.460
3	[9](D)	0.83 + i0.27	5.43840	74.9154	-0.387884	8.83448	0.449176	-654.504	8.0	-760.560
4	[9](A)	0.87+i0.27	4.35990	30.3941	-0.376959	8.96712	0.270940	-687.477	8.0	-618.431
5	[9](B)	1.05 + i0.27	2.04950	2.60222	-0.102332	9.71806	0.192626	-849.271	8.0	-236.559
6	[9](C)	1.07 + i0.26	1.99979	2.28184	-0.105698	9.76374	0.0702236	-861.215	8.0	-174.670

TABLE II: ηd scattering length (in fm) predicted by the seven separable potential models of the coupled ηN-πN-σN system. We give the results obtained including only η-exchange, η- and π-exchange, and η-π- and σ-exchange in the driving terms. Comparison with results of ref. [5] is provided on the lines labeled NR.

	Model	$a_{\eta N}$	η	$\eta+\pi$	$\eta+\pi+\sigma$
	0	0.42+i0.34	0.88+i1.34	0.39+i1.67	0.23+i1.68
NR	0	0.42+i0.34	1.01+i1.24	1.00+i1.28	0.99+i1.28
	1	0.72+i0.26	2.59+i1.84	2.67+i1.90	2.67+i1.90
NR	1	0.72+i0.26	2.53+i1.51	2.56+i1.51	2.57+i1.51
	2	0.75+i0.27	2.73+i1.66	2.78+i1.68	2.78+i1.68
NR	2	0.75+i0.27	2.75+i1.64	2.75+i1.62	2.76+i1.62
	3	0.83+i0.27	3.23+i1.88	3.28+i1.91	3.29+i1.91
NR	3	0.83+i0.27	3.28+i1.93	3.28+i1.91	3.30+i1.91
	4	0.87+i0.27	3.45+i1.92	3.50+i1.95	3.51+i1.95
NR	4	0.87+i0.27	3.55+i2.07	3.56+i2.05	3.57+i2.04
	5	1.05+i0.27	4.72+i2.47	4.80+i2.52	4.80+i2.52
NR	5	1.05+i0.27	4.91+i2.72	4.92+i2.70	4.93+i2.70
	6	1.07+i0.26	5.00+i2.54	5.09+i2.60	5.09+i2.60
NR	6	1.07+i0.26	4.77+i2.25	4.79+i2.25	4.79+i2.24